ELSEVIER

Biochimica et Biophysica Acta 1468 (2000) 87–98

BIOCHIMICA ET BIOPHYSICA ACTA

BBA

www.elsevier.com/locate/bba

Effect of influenza hemagglutinin fusion peptide on lamellar/inverted phase transitions in dipalmitoleoylphosphatidylethanolamine: implications for membrane fusion mechanisms

D.P. Siegel [a], R.M. Epand [b,*]

[a] *Department of Chemistry, The Ohio State University, 100 West 18th Avenue, Columbus, OH 43210, USA*
[b] *Department of Biochemistry, McMaster University, 1200 Main St. West, Hamilton, Ont. L8N 3Z5, Canada*

Received 13 April 2000; received in revised form 8 May 2000; accepted 24 May 2000

Abstract

Low mole fractions of viral fusion peptides induce inverted cubic (Q_{II}) phases in dipalmitoleoylphosphatidylethanolamine (DiPoPE), a lipid with unsaturated acyl chains that normally forms inverted hexagonal phase (H_{II}) above 43°C. The ability to form a Q_{II} phase is relevant to the study of membrane fusion: fusion occurs in liposomal systems under conditions where Q_{II} phase precursors form, and fusion may be an obligatory step in the lamellar (L_α)/Q_{II} phase transition. We used X-ray diffraction and time-resolved cryoelectron microscopy (TRC-TEM) to study the effects of the influenza hemagglutinin fusion peptide on the phase behavior and structure of DiPoPE. X-ray diffraction data show that at concentrations of 3–7 mol%, the fusion peptide (FP) induces formation of a Q_{II} phase in preference to the H_{II} phase. TRC-TEM data show that the FP acts at early stages in the phase transition (i.e. within seconds): at 2–7 mol%, FP decreases or inhibits formation of the L_α/H_{II} intermediate morphology observed via TRC-TEM in pure DiPoPE at the same temperature. Our X-ray diffraction data imply that FP either does not affect, or slightly increases, the spontaneous curvature of the host lipid (i.e. either does not affect or tends to destabilize inverted phases, respectively). FP may act in part by affecting the relative stability of two intermediate structures in the phase transition mechanism, as suggested previously. These results indicate a new way in which hydrophobic sequences of membrane proteins may be fusogenic.

1. Introduction

When added to phosphatidylethanolamines, low mole fractions of fusion peptides of some viral fusion proteins [1,2], as well as the amphipathic helical peptide alamethicin [3], induce Q_{II} phases that do not spontaneously form in the absence of the peptides. The mechanism of this peptide effect is of great interest because membrane fusion may be an obligatory step in the lamellar/inverted cubic (L_α/Q_{II}) phase transition [4,5], and the fusion peptides of viral proteins are critical for the membrane fusion activity of the proteins. Several authors have previously shown that viral fusion peptides increase the frequency of structures associated with the L_α/Q_{II} phase transition (e.g. [6–8]). Previously we used time-resolved cryoelectron microscopy (TRC-TEM) to study the intermediates in the L_α/inverted hexagonal (H_{II}) phase transition in large unilamellar vesicle (LUV) dispersions of DiPoPE [9]. In the present

* Corresponding author. Fax: +1-905-522-9033; E-mail: epand@fhs.csu.mcmaster.ca

0005-2736/00/$ – see front matter
PII: S0005-2736(00)00246-7

work, our aim is to determine how a well-studied viral fusion peptide affects the formation of the Q_{II} phase and of the early intermediates in this phase transition. In addition, we evaluated the relationships between these effects and membrane fusion processes.

2. Materials and methods

2.1. Materials

The phospholipid used in this study, dipalmitoleoyl phosphatidylethanolamine (DiPoPE), a lipid composed of 16:1 acyl chains, was purchased from Avanti Polar Lipids (Alabaster, AL), and used without further purification. The 20-amino acid N-terminal influenza fusion peptide (X31 strain of influenza virus; sequence GLFGAIAGFIENGWEGMIDG-amide) was made by standard solid phase synthetic methods using FMOC chemistry. The final purification of the peptide was on a Hamilton PRP-1 HPLC column. The peptide was applied to the column in a solution of DMSO, TFE, 0.1 M ammonium acetate (1:2:2, v/v/v) and the eluant was a gradient containing water, ammonium acetate and acetonitrile, with increasing acetonitrile concentrations. The fractions containing the purified peptide were then lyophilized to dryness. The identity of the peptide was verified by fast bombardment mass spectrometry and by amino acid analysis.

2.2. Preparation of peptide/DiPoPE LUVs

The fusion peptide (FP) was dissolved in methanol, and the FP concentration was determined on the basis of the tryptophan absorbance at 280 nm. (The extinction coefficient at 280 nm of Boc-Trp in methanol was verified as being 5550 M^{-1} cm^{-1}. This value was used for the extinction coefficient of FP.) An appropriate volume of this stock solution was mixed rapidly with a chloroform/methanol (3/1 v/v) solution of phospholipid. The volume of the phospholipid solution was equal to or greater than the peptide solution. The mixture was dried under vacuum in a rotary evaporator for 1 h, then hydrated in the glycine buffer (20 mM glycine, 150 mM NaCl, 0.2 mM EDTA, pH 9.6) to yield a lipid concentration of 1.1 mg/ml and then subjected to three freeze/thaw cycles (dry ice/room temperature water). The pH was measured after the freeze/thaw cycles and adjusted if necessary. The suspension was then extruded ten times, using two 100-nm polycarbonate filters (Nucleopore, Pleasanton, CA) in a stainless steel barrel extruder (Lipex Biomembranes, Vancouver, BC). The filters of the extruder usually clogged during the first extrusion: a pressure of up to 700 psi was necessary to extrude. After replacement of the filters and filter support, subsequent extrusion was facile (300 psi). The pH was checked again after extrusion. The FP concentration of the final LUV dispersion was estimated on the basis of the tryptophan absorbance using a PE LUV or buffer blank. Approximately 0.3 mg of the FP was lost on the filters and filter support, at each of several peptide concentrations. In calculating the peptide/lipid ratio, it was assumed that no lipid was lost on the filters. The nominal total mole percent of FP is calculated on a lipid basis, and is accurate to within about $\pm 0.4\%$ at 2 mol%, and ± 1 mol% at higher concentrations. The LUV preparation was stored on ice or in the refrigerator, sealed under Argon, until used (generally within 24 h).

2.3. Preparation of LUVs for differential scanning calorimetry (DSC)

This followed roughly the same procedure as for FP/DiPoPE LUVs (see above), except that no peptide was added and the lipid was dried down from a chloroform solution. The final lipid concentration was made to 2.2 mg lipid/ml.

2.4. DSC

A sample of DiPoPE LUVs was loaded into a sample cell of a Nano Differential Scanning Calorimeter (CSC Sciences, Provo, UT) which had been precooled to 0°C. It was acidified inside the sample cell of a DSC using an equal volume of ice-cold 50 mM acetate buffer, 120 mM NaCl, 0.1 mM EDTA, pH 4.5. The final pH of the acidified lipid was 5.0. The features of the design of the Nano Differential Scanning Calorimeter have been described [10]. The two solutions were separately degassed under vacuum, on ice, prior to loading in the calorimeter cells.

2.5. Preparation of samples for X-ray diffraction

A dilute solution of the influenza fusion peptide was made in methanol. The solution was sometimes slightly hazy. It was then mixed with a solution of DiPoPE in $CHCl_3$/MeOH (2/1; v/v) at which point the mixture became more transparent. A portion of the solvent was evaporated and the remaining solution was transferred to an X-ray capillary. The remainder of the solvent was then evaporated and last traces of solvent removed overnight under vacuum. The resulting deposit, containing 10 mg of lipid, was hydrated with 20 μl of buffer at pH 5.0 containing 50 mM acetate, 20 mM glycine, 135 mM NaCl and 0.15 mM EDTA. This buffer corresponds to the pH and composition of the final buffer suspending the lipid in TRC-TEM experiments (see below). The resulting paste was mechanically mixed with a fine metal wire and brought to the bottom of the capillary by centrifugation. The sample was put under Argon and the capillary was sealed and allowed to equilibrate several hours at room temperature.

2.6. X-ray diffraction experiments

A Rigaku-Denki (Model RU-200B) rotating anode was used to obtain nickel-filtered Cu Kα radiation of $\lambda = 1.54$ Å. X-rays were focused using a Frank's type camera and recorded with a TEC (Model 205) position sensitive proportional counter [11]. Calibration was done with freshly recrystallized samples of nonadecane, taking the spacings for this standard as 26.2 Å. Unoriented samples were measured in 1.5 mm outer-diameter glass capillaries. The specimen temperature was controlled to ±0.5°C with a thermoelectric device. The specimens were allowed to equilibrate at each temperature for at least 10 min and the diffraction collected over a period in the range of 20–200 min. Generally, cubic phases required longer collection times because of the weak intensity of the diffraction. The measured d-spacing is calculated from the average of all easily resolvable orders. Reported spacings are accurate to ±0.5 Å for lattices up to about 80 Å and to ±2 Å for larger lattices.

Table 1
X-ray diffraction results for pure DiPoPE

Temperature (°C)	Phase(s) present	Unit cell (nm)
25	L	4.92
35	L	4.82
	H_{II} (very weak)	7.09
42	H_{II}	7.04
46	H_{II}	6.93
55	H_{II}	6.80
65	H_{II}	6.60
Re-cooled to 25	L	4.91

Note: in all the tables, L stands for lamellar (L_α) phase, H_{II} for inverted hexagonal phase, and Q_{II} for inverted cubic phase. Also, the unit cell constant for the H_{II} phase is given as the diameter of the H_{II} tubes ($= 2d_{10}/\sqrt{3}$).

2.7. TRC-TEM

The same methods were used as in [9], except that a Philips CM-120 microscope with an accelerating voltage of 120 kV, a 70-μm objective aperture, and a Gatan cold stage (which maintained the specimens at −180°C) were used. EM grids (300-mesh copper with a lacy carbon film; Ted Pella) were mounted in a CEVS [12] at a temperature constant to within ±1°C and a relative humidity near 100%. A 4-μl drop of LUV suspension was placed on a TEM grid using a micropipetor. A second 4-μl drop of low-pH buffer, 120 mM NaCl, 50 mM sodium acetate, pH 4.5, 0.1 mM EDTA, was then mixed with it. The grid was blotted to form a thin aqueous film, and the grid was immediately plunged into liquid ethane. (It was confirmed that mixing equal volumes of glycine and acetate buffers yields a final pH of 5, and that the pH is still 5.5 even if the buffers are mixed in a 5/4 glycine/acetate volume ratio.) The grid was loaded into the cold stage under liquid N_2 and examined via TEM. Kodak SO-163 film was used and was developed in D-19 for 12 min. An underfocus of ‘1.7 μm was set for most exposures, though ‘1.9 μm was used for some images of the pH 9.6 dispersions.

3. Results and discussion

3.1. X-ray diffraction

Typical one-dimensional X-ray diffraction patterns of DiPoPE with and without FP, collected at 55°C, are shown (Fig. 1). The top curve of pure DiPoPE

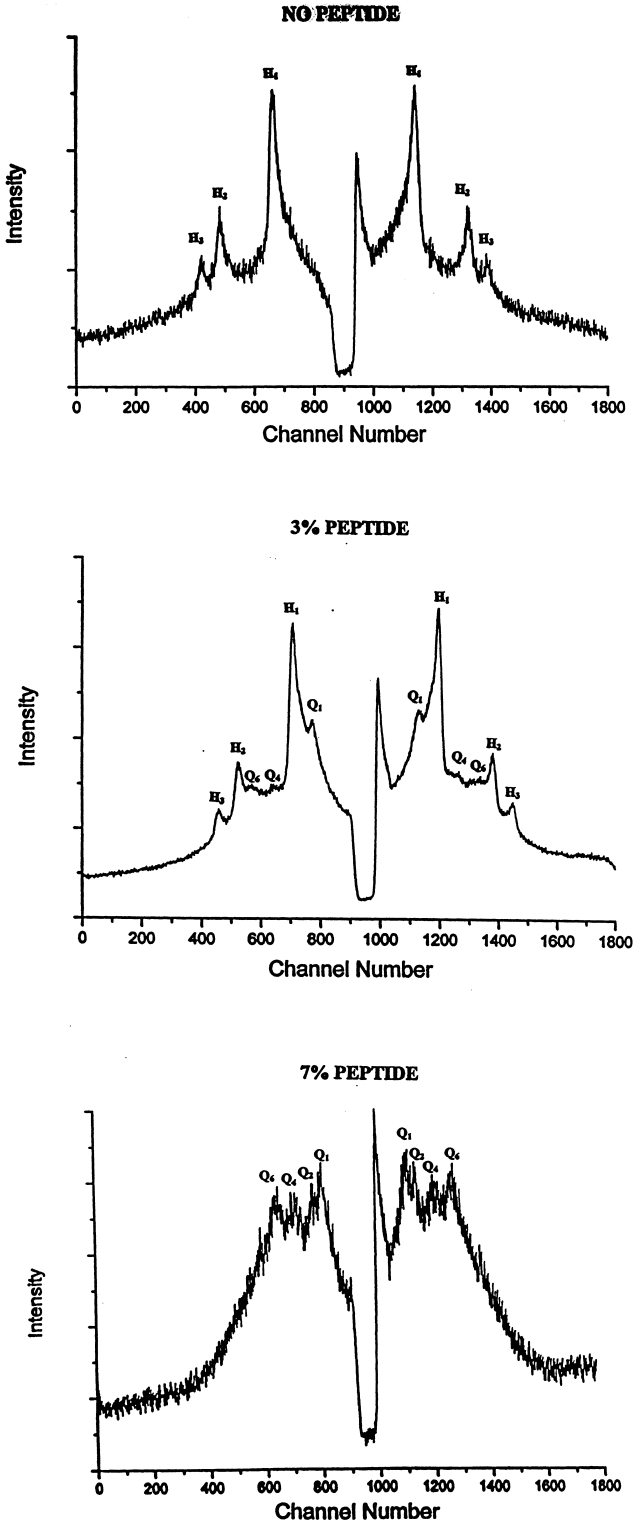

Fig. 1. One-dimensional diffraction patterns obtained from pure DiPoPE and FP/DiPoPE mixtures at 55°C. Top: pure DiPoPE. Middle: DiPoPE containing 3 mol% FP. Bottom: DiPoPE containing 7 mol% FP.

shows only the first three reflections from an H_{II} phase. The middle curve, of DiPoPE containing 3 mol% FP, shows reflections due to the H_{II} phase along with weaker reflections from a Q_{II} phase. The bottom diffractogram is from DiPoPE containing 7 mol% FP, and shows only reflections from a Q_{II} phase. Data collected from samples of different peptide concentrations are collated in Tables 1–3. The data in Table 1 were collected from a single sample of pure DiPoPE as a function of increasing temperature, as described in Section 2. The data are consistent with the occurrence of an L_α/H_{II} phase transition at a temperature between 35 and 42°C, consistent with past observations (e.g. [9,13]). The unit cell dimensions (L_α phase, bilayer repeat spacing; H_{II} phase, H_{II} tube diameter) were determined from the first lamellar reflection and the first three H_{II} reflections, respectively, in all cases. This lipid does not form an L_β phase in liquid water. When the sample was cooled back to 25°C from 65°C, the transition reversed to produce only the L_α phase. Diffraction results from a sample containing 3 mol% FP in DiPoPE are listed in Table 2. Here the behavior is obviously different. The temperature of the L_α/H_{II} phase transition is broadened to higher temperatures, occurring between 36 and 55°C. Traces of a Q_{II} phase were observed in this sample starting at 55°C. Since only one long spacing was observed (at ca. 8.5 nm), the assignment is tentative. However, at 65°C, four reflections are observed that index as a Pn3m Q_{II} phase. Evidence for a Q_{II} phase has previously been observed in DiPoPE containing 1 mol% of the same peptide at a similar temperature [2], and this same type of Q_{II} phase can be induced in some pure phosphatidylethanolamine systems by temperature-cycling [14,15]. Upon cooling to 25°C, weak reflections corresponding to Q_{II} and L_α phase lattices were observed. Similar phase behavior was observed in a sample containing 3.2 mol% FP. Interestingly, this sample was heated more rapidly (a smaller number of steps at larger temperature intervals), and only a weaker, single reflection from a Q_{II} lattice was observed (data not shown). Both of these latter two sets of observations are consistent with the sluggish kinetics and hysteresis often observed in L_α/Q_{II} phase transitions in phosphatidylethanolamine (PE) and PE-derivative systems [14–18], as well as in a PE

Table 2
X-ray diffraction results for 3 mol% FP in DiPoPE

Temperature (°C)	Phase(s) present	Unit cell (nm)	Comments
13–27.5	L	5.09–5.10	
36	L	5.13	
	H_{II}	7.19	
39	L	5.19	
	H_{II}	7.21	
42	L (minor)	5.09	
	H_{II}	7.09	
45	L (trace)	4.95	
	H_{II}	7.03	
50	L (trace)	4.87	
	H_{II}	6.92	
55	H_{II}	6.85	Only one reflection for Q_{II} (assumed Pn3m)
	Q_{II}	12.0	
65	H_{II}	6.69	Four of the first five reflections indexing as a Pn3m phase ($\sqrt{2}$, $\sqrt{3}$, $\sqrt{6}$, and $\sqrt{8}$)
	Q_{II} (Pn3m)	11.4	
Re-cooled to 25	L	5.16	Only one reflection for the putative Q_{II} phase. The L and Q_{II} reflections are weak and broad
	Q_{II} (?)	13	

derivative that also contained low concentrations of hydrophobic peptides [19].

Results of X-ray diffraction experiments on samples containing 7 mol% FP are shown in Table 3. In this case, the reflections were too broad to reliably determine the lattice constants of the L_α and H_{II} phases. Only L_α phase reflections were observed at low temperatures, a broad L_α/H_{II} transition commenced at around 41°C and lasted at least until 47°C, and traces of a Pn3m Q_{II} lattice appeared at 41°C, becoming well-defined at 50°C and higher temperatures. This is very similar to the phase behavior observed in the 3 mol% FP sample (Table 2). Hence it is clear that low concentrations of FP are capable of inducing formation of a Pn3m Q_{II} phase that does not form in pure DiPoPE under the same circum-

Table 3
X-ray diffraction results for 7 mol% FP in DiPoPE

Temperature (°C)	Phase(s) present	Unit cell (nm)	Comments
25	L	5.31	
30	L	5.30	
35	L	5.33	
38	L	5.34	
41	L/H_{II} (?)	?	A single broad reflection at 5.75 nm may include both L and H_{II} phase reflections. Only a single Q_{II} reflection observed (10.9 nm)
	Q_{II} (?)	15.4	
43	L/H_{II} (?)	?	As above: for L and H_{II}, only a single broad reflection was observed at 5.58 nm
	Q_{II} (?)	15.8	
47	L/H_{II} (?)	?	As above: for L and H_{II}, only a single broad reflection was observed at 5.40 nm
	Q_{II} (?)	15.3	
50	Q_{II} (Pn3m)	14.4	Four reflections indexing as a Pn3m Q_{II} lattice
55	Q_{II} (Pn3m)	13.6	Four reflections indexing as a Pn3m Q_{II} lattice
60	Q_{II} (Pn3m)	12.3	Four reflections indexing as a Pn3m Q_{II} lattice

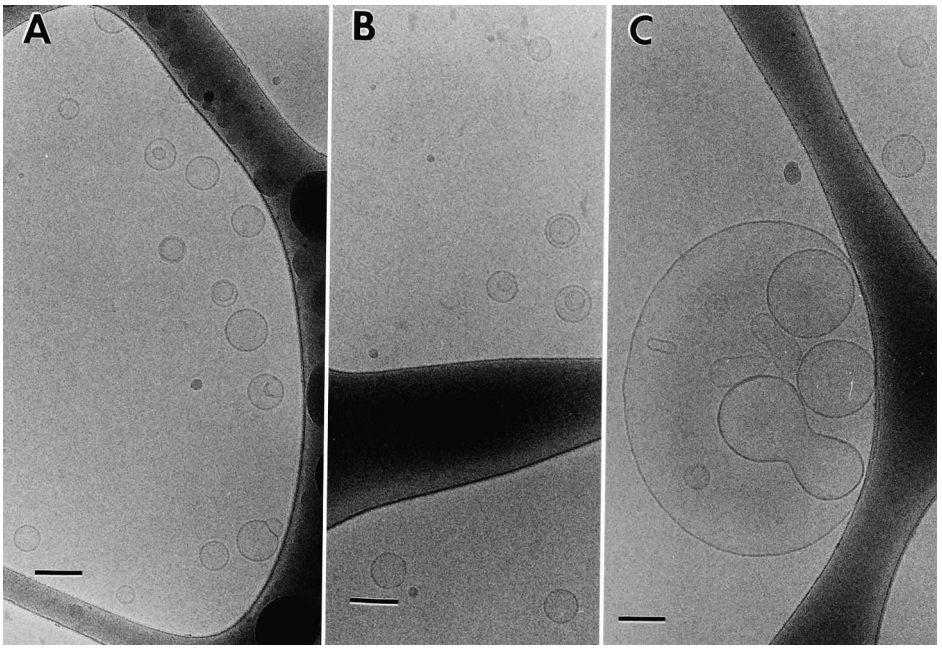

Fig. 2. Micrographs of DiPoPE and FP/DiPoPE LUV dispersions at pH 9.6 quenched from 26°C. (A) DiPoPE LUVs produced using the same protocol as for the FP/DiPoPE LUVs used in this work. The large black regions are strands of a lacy graphite film that supports the aqueous films. The predominant structures are LUVs about 40–70 nm in diameter. (B) FP/DiPoPE LUVs with 7 mol% FP. Most of the structures are LUVs similar in size to those in (A), although some of the LUVs appear to have invaginated. (C) FP/DiPoPE LUV dispersion with 7 mol% FP after 18 days of storage at 4°C. This field emphasizes the presence of a subpopulation of larger vesicles, often consisting of oligolamellar vesicles or several vesicles enveloped by a larger one. Scale bars: 100 nm.

stances. Recent experience with Q_{II} phases in both pure lipid [15,17,18] and peptide–lipid [19] systems suggests that the lattice constants of the first Q_{II} phases to form either with increasing temperature or increasing incubation time at a constant temperature can initially be much larger than the values measured here. It is possible that Q_{II} phases might be forming at lower temperatures in this system, with the lowest-angle (and most easily observable) reflections occurring at angles too small to be detected by the present apparatus.

Inspection of Tables 1–3 shows that addition of FP at low concentrations increases the interlamellar spacing in the L_α phase relative to pure DiPoPE, by as much as 0.4 nm at 7 mol%. Interestingly, the lattice constant of the H_{II} phase at 45°C is almost the same in the 3 mol% FP samples as in the pure DiPoPE sample (to within 0.1 nm). Therefore, the peptide is either not partitioning into the H_{II} phase, or is not affecting the spontaneous radius of curvature of the DiPoPE host lipid, or there are counterbalancing effects of electrostatic repulsion by the peptide increasing the spontaneous curvature, while other peptide–lipid interactions decrease it. However, in general, the equilibrium H_{II} tube diameter would be expected to change if the peptide changed the spontaneous curvature of DiPoPE [20,21]: an increment in spontaneous curvature would be observed as an increment in H_{II} tube diameter. The addition of 7 mol% of FP increases the onset temperature for formation of H_{II} phase, which shows that the FP is not phase separating into a peptide-rich lamellar phase at lower temperatures, but increases the L_α/H_{II} phase transition temperature of a uniform lipid/FP mixture. A reduction in spontaneous curvature would be expected to decrease the onset temperature [21]. Together, these two observations show that, in this concentration range, the FP does not stabilize nonlamellar phases by reducing the spontaneous radius of curvature of the host lipid. This is in contrast to results obtained at lower fusion peptide concentrations in this [7] and other systems (e.g. [8,22]). If anything, there is a small increase in spontaneous curvature (i.e. favoring lamellar phase formation), judging from the comparison of H_{II} tube diameters at constant temperature in Tables 1 and 2.

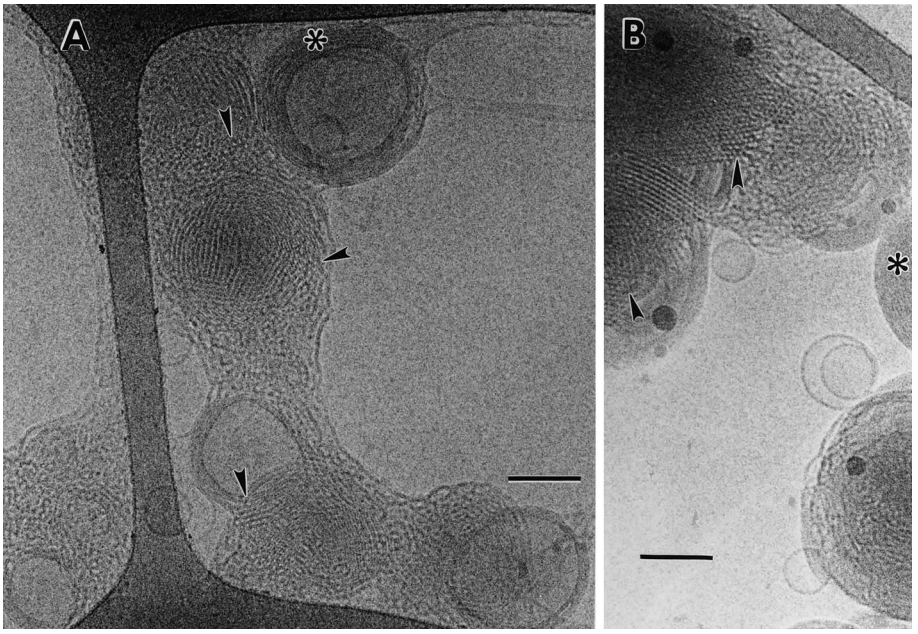

Fig. 3. DiPoPE LUVs that were neutralized with acetate buffer at a temperature of 31°C, seconds before vitrification. (A) At the left of the figure, many poorly ordered interconnections between lamellae are visible. These are probably TMCs [4,5,9]. Arrowheads: regions in which quasihexagonal structure has formed. This may correspond to the ordered TMC array postulated as an H_{II} phase precursor [4,5,9]. Asterisk: a multilamellar vesicle (MLV). MLVs also form in these dispersions, and represent the equilibrium structure at this temperature, as demonstrated by X-ray diffraction (Table 1) and time-resolved NMR measurements [9]. (B) Same sample composition and temperature. Arrowheads: regions of better-ordered quasihexagonal structure than in (A). Asterisk: edge of an MLV.

3.2. TRC-TEM data

Fig. 2 shows micrographs of DiPoPE and FP/DiPoPE dispersions at pH 9.6, quench frozen from 26°C. Fig. 2A is a micrograph of a dispersion of DiPoPE LUVs produced by the same method used to generate FP/DiPoPE LUVs. The large black regions are strands of the lacy graphite film that supports the thin aqueous films prior to vitrification. The structures visible in the vitrified films are predominantly LUVs with diameters of 40–70 nm. Fig. 2B shows FP/DiPoPE LUVs with 7 mol% FP. Most of the structures in these images are also LUVs, some of which appear to have invaginated. The specimen in Fig. 2B was made from an LUV dispersion 3 days after production. However, the specimen in Fig. 2C was made from an 18-day-old LUV dispersion. In this sample, there was a substantial subpopulation of larger structures that are several tenths of a micron in diameter, often consisting of several vesicles enveloped by a larger one, or of oligolamellar vesicles in which the enclosed structures have comparable diameters. This growth in size of the lipid aggregates might have been influenced by the accumulation of lipid hydrolysis products (see 'DSC Data', below).

Fig. 3 shows TRC-TEM images of specimens of DiPoPE LUVs that were neutralized with acetate buffer at a temperature of 31°C, seconds before vitrification. The midpoint of the L_α/H_{II} transition of freshly prepared, pH-neutralized DiPoPE LUVs as determined via DSC (see below) is 42°C. The same intermediate morphology was observed as in [9], and in both cases this morphology formed well below the equilibrium T_H. LUVs rearrange into large structures, with different types of interlamellar connections. At the left of Fig. 3A, many poorly ordered interconnections between lamellae are visible. These are probably transmonolayer contacts (TMCs; [4,5,9]). The arrowheads indicate regions in which quasihexagonal (QH) structure has formed: this may correspond to the ordered TMC array postulated in [9], as an intermediate in the L_α/H_{II} phase transition. It is observed in DiPoPE only when the

temperature is approximately 20°C below T_H or higher. Catenoidal interlamellar attachments (ILAs, [4,5,9]) are occasionally visible at the periphery of some membrane assemblies. Fig. 3B is another image of DiPoPE at pH 5 and 31°C. The arrowheads indicate larger regions of better-ordered quasihexagonal structure, and the asterisk again indicates an MLV. Despite the abundance of non-lamellar structures in Fig. 3B,C, the L_α phase is the equilibrium phase at 31°C, and time-resolved NMR measurements [9] show that the non-lamellar morphology that forms under these circumstances is transient, with only lamellar phase DiPoPE being present within about 1–2 min after neutralization. The specimens in Fig. 3 were made using LUV dispersions produced less than 24 h before specimen vitrification.

Fig. 4A–D are micrographs of FP/DiPoPE dispersions with different concentrations of FP, neutralized seconds before vitrification, at the same temperature as the pure DiPoPE specimens in Fig. 3 (31°C). In Fig. 4A, the FP concentration was 2 mol%. The QH domains that are abundant in the DiPoPE LUV dispersion are still visible, but are very infrequent in this sample (not shown). The most common lipidic structures are MLVs. There are small and infrequent inclusions of disordered intermediates, but these are much rarer than in pure DiPoPE under the same conditions. Fig. 4B is a micrograph of a neutralized dispersion of 5 mol% FP in DiPoPE. The most common structures are LUVs and a few oligolamellar vesicles. There are many fewer MLVs than in 2 mol% FP specimens. Most of the specimens consisted of LUVs that were not extensively aggregated. A denser-than-usual region was deliberately selected here to emphasize the small change in LUV size and structure in the presence of 5 mol% FP. Fig. 4C and D are micrographs of 7 mol% FP/DiPoPE dispersions treated in the same way. Obviously, a further increase in peptide concentration did not substantially change the morphology observed at 5 mol%, except that MLVs are even rarer at 7 mol%. At both 5 and 7 mol% FP, there are infrequent examples of small clusters of disordered intermediates. Fig. 4A–D were made from LUV dispersions that had been stored for less than 24 h at 4°C at the time of specimen vitrification.

Fig. 4E is a micrograph of a neutralized 15 mol% FP/DiPoPE dispersion, that was vitrified at a lower temperature of only 25°C. At this, the highest FP concentration we investigated, domains of disordered intermediates were more frequent and larger in size than at 2–7 mol%, despite the fact that the temperature was lower. Many clear examples of ILAs are seen in profile at the periphery of these domains. However, it is important to note that this specimen was made from an LUV dispersion that had been stored for 6 days at 4°C: it is possible that extensive hydrolysis of the DiPoPE during this time lowered the T_H value and also contributed to the more extensive intermediate formation in this specimen (see below, under 'DSC Data'). It is shown here to emphasize the existence of ILAs in such dispersions, which are Q_{II} phase precursors [17].

The TRC-TEM data in Fig. 4 allow two conclusions concerning the effect of FP on inverted phase formation. First, when FP/DiPoPE and DiPoPE systems are compared at constant temperature, the intermediate morphology associated with the L_α/H_{II} phase transition [9] is rarer (2–3 mol%) or absent (7 mol%) in the FP/DiPoPE specimens. This is consistent with the X-ray diffraction data (Tables 1 and 2), which show that addition of FP at 2 or 3 mol% broadens the lamellar/non-lamellar transition to higher temperatures, and, at 7 mol%, increases the onset temperature for inverted phase formation. Second, FP acts at an early stage in the lamellar/inverted phase transition. At 2–3 mol% FP, where the onset temperature of the lamellar/non-lamellar phase transition is nearly the same as in pure DiPoPE (Tables 1 and 2), FP reduces the extent of formation of intermediates in the L_α/H_{II} and L_α/Q_{II} transitions relative to pure DiPoPE within the first few seconds after the transition is triggered. This is consistent with our earlier hypothesis [5,9] that hydrophobic peptides like FP could induce Q_{II} phase formation, and decrease the rate and/or extent of H_{II} phase formation. Few L_α/Q_{II} transition intermediates (ILAs) are visible in Fig. 4A–D because these images were obtained within seconds after the pH was dropped, and the L_α/Q_{II} phase transition is notoriously slow (hours) and hysteretic (e.g. [14,16–19]). However, it is also possible that the peptide slows intermediate formation by hindering close apposition of the L_α phase bilayers, which would slow formation of the intermembrane intermediates. This could reduce the rate of the transitions at constant temperature, and post-

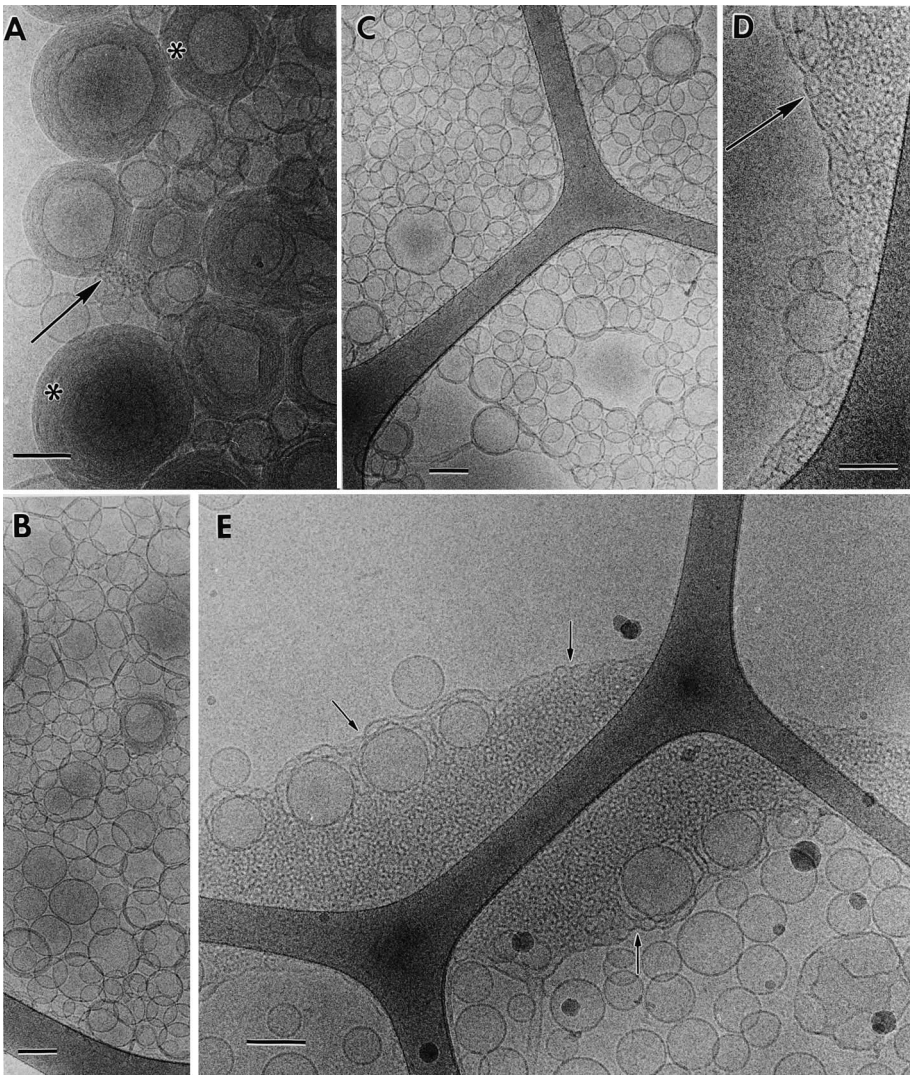

Fig. 4. DiPoPE LUV dispersions containing different concentrations of FP, all acidified to pH 5 before vitrification. (A) 2 mol% FP, 31°C. The QH domains and inclusions of disordered intermediates (arrow), that are common in pure DiPoPE dispersions at the same temperature (Fig. 3), are rare in this sample. The most common structures are MLVs (asterisks). (B) 5 mol% FP, 31°C. in DiPoPE. At this higher FP concentration, the most common structures are LUVs and a few oligolamellar vesicles. There are also many fewer MLVs than in 2 mol% FP specimens. Most of the specimens showed dispersed LUVs. A denser-than-usual field was selected here to emphasize the small change in LUV size and structure. (C and D) 7 mol% FP, 33°C. The same sort of morphology is observed as at 5 mol% FP, except that MLVs are even rarer. Small clusters of disordered intermediates (arrow) are infrequently observed, as at 5 mol% FP. (E) 15 mol% FP, 25°C. Domains of disordered intermediates (center of figure) are more common and larger than in A–D. Many examples of ILAs are visible (small arrows). However, this specimen was made from an LUV dispersion that had been stored for 6 days at 4°C. Chemical degradation of DiPoPE in this case may have produced structures that would not normally occur (see text).

pone rapid formation of intermediates until higher temperatures, since the rate and extent of intermediate formation should increase with increasing temperature [4,5]. Such an effect would be consistent with the increase in L_α phase interlamellar spacing observed in the presence of FP (Tables 1–3).

3.3. DSC data

In order to prepare LUVs from PE, the lipid suspension must first be brought to alkaline pH. In some cases, the LUVs were maintained in alkaline solution after extrusion so that they would be avail-

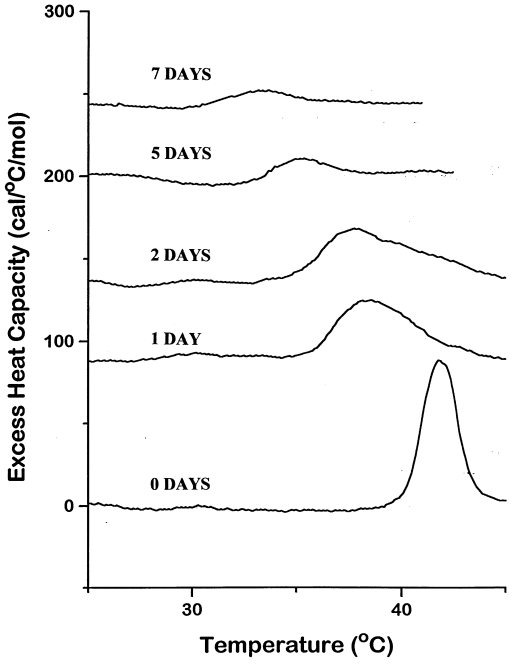

Fig. 5. DSC thermograms of acidified DiPoPE LUV dispersions. DiPoPE LUVs were stored for the times indicated on each of the traces at 4°C, before being acidified inside the DSC cell at a temperature near 0°C, and then scanned.

able for the TRC-TEM. We had some concerns about the chemical stability of the DiPoPE that was stored at pH 9.6, even though it was kept at 4°C in this work and in the TRC-TEM work on pure DiPoPE reported earlier [9]. We assessed the rate of formation of impurities that lowered T_H as a function of the time of storage at pH 9.6 at 4°C. At appropriate times, samples of the LUVs were withdrawn and loaded into the DSC (pre-cooled to 0°C), and the LUV dispersions were neutralized with an equal volume of cold acetate buffer (to decrease the pH to 5 and enable the phase transition at higher temperatures). Then the DSC experiment was performed. DSC data from thermograms obtained immediately after production, and at times 24, 48, 120, and 168 h after production, are displayed in Fig. 5. The peak temperature of the endotherm drops by a total of 3.5°C after 1 day, 4°C after 2 days, 7°C after 5 days, and more than 8°C after 7 days. The enthalpy of the transitions drops rapidly after the first 5 days. However, it is clear that LUVs used within 24 h after production have a T_H that is the same to within 3.5°C of freshly produced lipid.

In the present work, LUV dispersions were used within 1–3 days after production, except as otherwise noted in the figure captions. Dynamic morphological results on pure DiPoPE (Fig. 3A,B) and FP/DiPoPE (Fig. 4A–D) dispersions were obtained on samples that were less than 1 day old. In the work reported in [9], LUV dispersions were used within 6–8 days of production, and occasionally within 1 day. While the samples kept for 6–8 days probably had transition temperatures that were as much as 8°C lower than in freshly prepared LUVs, it is important to note that the relevant dynamic morphologies associated with transition intermediates was observed at temperatures more than 22–38°C below the original value of T_H [9]. In addition, the same dynamic morphology was also observed in specimens prepared from LUV dispersions that were less than 1 day old (i.e. in Figs. 1D,G and 3C of [9]), at temperatures 16–38°C below T_H. These results cannot be explained in terms of a reduction in T_H due to DiPoPE hydrolysis. Moreover, control experiments on pure DiPoPE were performed for the present paper (Fig. 3A,B) using LUV dispersions produced less than 24 h of use, and generated the same morphological results as observed in [9].

Therefore, the principal results of the morphological study in [9] and in Figs. 3 and 4 of the present work are not due to H_{II} phases forming at a lower than expected transition temperature. It is possible that the hydrolysis products formed by DiPoPE degradation may play a role in forming some of the intermediate morphology in DiPoPE systems. Thin-layer chromatography results (not shown) show that about 3% of the DiPoPE in LUVs hydrolyzes after 24 h of storage in glycine buffer at 4°C. However, it should be noted that disordered intermediate arrays and ILAs as imaged in Figs. 3 and 4 are *not* created only in samples where lipid hydrolysis has occurred. The same structures have been observed in large numbers via freeze-fracture TEM (e.g. [23]) and via TRC-TEM [9,24,25] in temperature-jumped DOPE-Me LUV dispersions that were made and stored on ice at pH 7.4. These are conditions under which lipid degradation does not occur.

4. Conclusions

This research produced three principal results.

First, the addition of 3–7 mol% of FP, the fusion peptide of influenza hemagglutinin, to DiPoPE induces Q_{II} phase formation along with H_{II} phase, whereas the Q_{II} phase is not observed in the pure lipid system under the same circumstances. This is demonstrated by the observation of Q_{II} phase X-ray diffraction patterns in the FP/DiPoPE system and not in pure DiPoPE incubated under the same conditions (Fig. 1, Tables 1 and 2).

Second, the TRC-TEM shows that effect of FP occurs very early in the overall transition process, which was described in earlier TRC-TEM research [9,24,25]: addition of 2–7 mol% FP inhibits the formation of intermembrane intermediates in the phase transition when the systems are compared at a temperature where intermediate morphology is abundant in pure DiPoPE (Figs. 2–4).

Third, the X-ray diffraction data show that FP does not decrease the spontaneous radius of curvature of the lipid system and, if anything, slightly increases it (Table 3). This is in contrast with earlier research that reported that viral fusion peptides at lower concentrations decreased the spontaneous curvature of the host lipid system, and induced nonlamellar phases at lower temperatures than observed in the pure lipid system [7,8,22]. Clearly, in this system, in the concentration range of 2–7 mol%, the peptides have a very different effect. These two observations, however, are not necessarily contradictory. One possibility is that there is more self-associated peptide in the membrane at the higher peptide mole fractions used in the present study and that these peptide oligomers have a different effect on T_H than do peptide monomers in the membrane. The other consideration is that the interconversion between H_{II} and Q_{II} phases can exhibit very slow kinetics. In the earlier work at low peptide concentration, there is very little Q_{II} phase formed and the transition from the L_α to H_{II} phase is observed, while at high peptide concentration the most predominant phases are the L_α and Q_{II} phases and it is not possible to measure T_H. The temperature of conversion to the cubic phase may not be solely dependent on membrane curvature.

The mechanism by which FP produces Q_{II} phase in preference to H_{II} phase in DiPoPE is not clear. Earlier [9], we suggested that hydrophobic peptides, like FP might favor production of ILAs (fusion pores, which are Q_{II} phase precursors) from critical intermediates know as transmonolayer contacts (TMCs). This could come about if the membrane-absorbed peptides lowered the rupture tension of the DiPoPE bilayers. If the central bilayer diaphragm of a TMC ruptures, it forms an ILA. If the diaphragm is stable, the TMCs can live long enough to aggregate with other TMCs to form H_{II} phase precursors [5,9]. It has been shown that incubation of lipid vesicles with aqueous solutions containing FP does in fact lower the rupture tension substantially (by ca. 60% or more; [26]). Rupture of TMCs to form ILAs would both delay TMC aggregation into H_{II} precursors and make ILAs available to assemble into Q_{II} phase lattices [5], which do not occur in the pure lipid. In addition, the presence of ILAs in multilamellar aggregates should also hinder H_{II} phase formation [5]. Therefore, our observations, and those of Longo et al. [26], are quite consistent with our hypothesis that FP induces Q_{II} phase formation by lowering the membrane rupture tension and destabilizing TMCs.

Hydrophobic peptides could conceivably increase membrane fusion rates in vivo via the same sort of mechanism, which is thought to involve similar types of lipid intermediates. However, with regard to the role of FP in influenza hemagglutinin-mediated fusion, it must be noted that the fusion peptide would have to access the diaphragm of the TMC from within the virus or the cytoplasmic side of the target cell membrane in order to have the effect we postulate. In vivo the fusion peptide can only enter the fusion intermediate from outside of the hypothetical TMC (i.e. from the extracellular space). The FP can only have access to the membrane diaphragm of the TMC if it can somehow traverse the exterior monolayers of the fusion intermediate. Thus it is not clear that this behavior of FP is relevant to the mechanism of viral protein-induced membrane fusion. However, it is possible that the hydrophobic portions of other proteins, or perhaps the intra-viral domains of fusion catalyzing proteins or of neighboring proteins, could be fusogenic through this type of mechanism.

Acknowledgements

We acknowledge support from the Medical Re-

search Council of Canada, Grant MT-7654, and the NIH Grant GM56969. We are also grateful to Dr. Raquel Epand for her assistance and to Drs. Sek Wen Hui and Ari Sen for use of their diffraction equipment. The influenza fusion peptide was synthesized by John W. Hawes.

References

[1] A. Colotto, I. Martin, J.-M. Ruysschaert, A. Sen, S.W. Hui, R.M. Epand, Biochemistry 35 (1996) 980–989.
[2] A. Colotto, R.M. Epand, Biochemistry 36 (1997) 7644–7651.
[3] S.L. Keller, S.M. Gruner, K. Gawrisch, Biochim. Biophys. Acta 1278 (1996) 241–246.
[4] D.P. Siegel, Biophys. J. 65 (1993) 2124–2140.
[5] D.P. Siegel, Biophys. J. 76 (1999) 291–313.
[6] P.L. Yeagle, R.M. Epand, C.D. Richardson, T.D. Flanagan, Biochim. Biophys. Acta 1065 (1991) 49–53.
[7] R.M. Epand, R.F. Epand, Biochem. Biophys. Res. Commun. 202 (1994) 1420–1425.
[8] S.M. Davies, R.F. Epand, J.P. Bradshaw, R.M. Epand, Biochemistry 37 (1998) 5720–5729.
[9] D.P. Siegel, R.M. Epand, Biophys. J. 73 (1997) 3089–3111.
[10] G. Privalov, V. Kavina, E. Freire, P.L. Privalov, Analyt. Biochem. 232 (1995) 79–85.
[11] A. Sen, S.W. Hui, D.A. Mannock, R.N. Lewis, R.N. McElhaney, Biochemistry 29 (1990) 7799–7804.
[12] J.R. Bellare, H.T. Davis, L.E. Scriven, Y. Talmon, J. Electron Microsc. Tech. 10 (1988) 87–111.
[13] R.M. Epand, Chem. Phys. Lipids 52 (1990) 227–230.
[14] E. Shyamsunder, S.M. Gruner, M.W. Tate, D.C. Turner, P.T.C. So, C.P.S. Tilcock, Biochemistry 27 (1988) 2332–2336.
[15] B. Tenchov, R. Koynova, G. Rapp, Biophys. J. 75 (1998) 853–866.
[16] S.M. Gruner, M.W. Tate, G.L. Kirk, P.T.C. So, D.C. Turner, P.S. Tilcock, P.R. Cullis, Biochemistry 27 (1988) 2853–2866.
[17] D.P. Siegel, J.L. Banschbach, Biochemistry 29 (1990) 5975–5981.
[18] V.C. Cherezov, D.P. Siegel, M.C. Caffrey, manuscript in preparation.
[19] D.P. Siegel, V.C. Cherezov, D V. Greathouse, R. Koeppe II, J.A. Killian, M.C. Caffrey, manuscript in preparation.
[20] M.W. Tate, S.M. Gruner, Biochemistry 28 (1989) 4245–4253.
[21] M.M. Kozlov, S. Leikin, R.P. Rand, Biophys. J. 67 (1994) 1603–1611.
[22] R.F. Epand, I. Martin, J.-M. Ruyscchaert, R.M. Epand, Biochem. Biophys. Res. Commun. 295 (1994) 1938–1943.
[23] H. Ellens, D.P. Siegel, D. Alford, P.L. Yeagle, L. Boni, L.J. Lis, P.J. Quinn, J. Bentz, Biochemistry 28 (1989) 3692–3703.
[24] D.P. Siegel, J.L. Burns, M.H. Chestnut, Y. Talmon, Biophys. J. 66 (1989) 402–414.
[25] D.P. Siegel, W.J. Green, Y. Talmon, Biophys. J. 66 (1994) 402–414.
[26] M.L. Longo, A.J. Waring, D.A. Hammer, Biophys. J. 73 (1997) 1430–1439.